www.czasopisma.pan.pl PAN POLSKA AKADEMIA NAUK www.journals.pan.pl

Arch. Metall. Mater. **65** (2020), 1, 393-402

DOI: 10.24425/amm.2020.131742

SHIH-HSIEN CHANG[1*], CHIH-YAO CHANG[1], KUO-TSUNG HUANG[2]

STUDY ON THE SINTERED CHARACTERISTICS AND PROPERTIES OF Co-30 MASS% Cr ALLOYS UNDER VARIOUS VACUUM HOT-PRESS SINTERING TEMPERATURES AND PRESSURES

In this research, Co-30 mass% Cr alloys were fabricated by a vacuum hot-press sintering process. Different amounts of submicron cobalt and chromium (the mean grain size is 800 and 700 nm, respectively) powders were mixed by ball milling. Furthermore, this study imposed various hot-press sintering temperatures (1100, 1150, 1200 and 1250°C) and pressures (20, 35 and 50 MPa), while maintaining the sintering time at 1 h, respectively. The experimental results show that the optimum parameters of hot-press sintered Co-30 mass% Cr alloys are 1150°C at 35 MPa for 1 h. Meanwhile, the sintered density reaches 7.92 $g \cdot cm^{-3}$, the closed porosity decreases to 0.46%, and the hardness and transverse rupture strength (TRS) values increase to 77.2 HRA and 997.1 MPa, respectively. While the hot-press sintered Co-30 mass% Cr alloys at 1150°C and 20 MPa for 1 h, the electrical conductivity was slightly enhanced to 1.79×10^4 $S \cdot cm^{-1}$, and the phase transformation (FCC → HCP) of cobalt displayed a slight effect on sintering behaviors of Co-30 mass% Cr alloys. All these results confirm that the mechanical and electrical properties of Co-30 mass% Cr alloys are effectively improved by using the hot-press sintering technique.

Keywords: Co-30 mass% Cr alloys, hot-press sintering, hardness, TRS and electrical conductivity

1. Introduction

Cobalt based alloys are one of the most employed biomaterials for articulating hip and knee prosthesis due to their suitable combination of mechanical and tribological properties as well as the good corrosion resistance [1]. The excellent resistance of cobalt based alloys to wear and oxidation benefits from the solid solution hardening, oxidation and carbide precipitation hardening by adding tungsten, molybdenum, chromium and graphite elements [2]. Among them, chromium with iron and cobalt forms alloys is appreciated particularly due to their high oxidation, corrosion and heat resistance, as well as the excellent creep strength at high temperatures [3]. Hence, cobalt-chromium (CoCr) alloys are widely used for the fabrication of different types of mechanical parts, biomedical implants, like orthopedic joints and stents due to the high strength and good corrosion resistance [4-6]. However, the metal ions (such as Co and Cr) can produce carcinogenic effect which cannot be tolerated in large quantities of human body and cause harmful reactions leading to a foreign body reaction. Moreover, CoCr alloys are also used in electronic materials, such as the porcelain-fused-to-metal restorations. Thus, how to increase the hardness, strength and electrical properties of CoCr alloys and in turn reduce the release of metal ions is technologically and clinically important research topic [7,8].

In recent years, the investment casting process has been used to fabricate CoCr dental metallic restorations. However, increased tool and machine wear were caused by the high rigidity of the solid blank and high acquisition and maintenance costs pose significant disadvantages [9]. Furthermore, the microstructure and above-mentioned properties of CoCr alloys, in particular the mechanical properties, depend not only on the chemical composition but also on the manufacturing process. A recent development in the fabrication of CoCr alloy include: lost-wax casting, forging and powder metallurgy (P/M) [9,10]. While P/M techniques exhibit superior mechanical and chemical properties compared with the two other methods. It is a good method for fabrication of high melting material with better mechanical properties. Among them, sintering is a useful method for manufacturing parts from powders, by heating the material until its particles adhere to each other. But conventional sintered P/M-parts usually have more than 5% porosity. Whereby, enhanced sintering techniques can be applied to obtain higher densities and improved porosity in the sintered parts [2,10,11].

[1] NATIONAL TAIPEI UNIVERSITY OF TECHNOLOGY,DEPARTMENT OF MATERIALS AND MINERAL RESOURCES ENGINEERING, TAIPEI 10608, TAIWAN, ROC
[2] NATIONAL KANGSHAN AGRICULTURAL INDUSTRIAL SENIOR HIGH SCHOOL, DEPARTMENT OF AUTO-MECHANICS, KAOHSIUNG 82049, TAIWAN, ROC

* Corresponding author: changsh@ntut.edu.tw

How to fabricate as well as increase the hardness, strength and corrosion resistance of CoCr alloys is an important research topic. As mentioned previously, P/M technology is the conventional process for the production of CoCr alloys. Hot-press sintering is another special P/M technology, which directly press and sinter the material through a graphite mold to transmit the pressure to the powders [12]. Moreover, the compaction and sintering take place simultaneously. The hot pressing process can obtain the more dense material at relatively lower sintering temperature; whereby, it is a novel technique to produce the CoCr alloys [13-15].

Previous study indicated that hot pressing is a feasible technique for the production of CoCrMo compacts for biomedical applications with adequate mechanical properties. The mechanical strength, porosity and hardness can be adjusted by tuning the processing conditions [16]. Moreover, Sato et al. chose hot pressing in N_2-containing atmosphere as a production way for (P/M)-CoCrMo alloys. And reported some results on the mechanical properties of dense and porous CoCrMo compacts [17]. As for the mechanical and electrochemical properties for biomedical applications of the hot press sintered Co-30%Cr alloy are still unclear.

The aim of this investigation was the optimization of sintering microstructure and mechanical properties of Co-30 mass% Cr alloys by vacuum hot-press sintering temperatures and pressures. In this work, a CoCr alloy was produced by means of the vacuum hot-press sintering process and solid-phase sintering of P/M technology. The effects of submicron-structured powders and hot-press sintering temperatures and pressures on the Co-30 mass% Cr alloys were our chief concern. A series of experiments on the hot-press sintered specimens were simultaneously carried out to explore the sintering behaviors and properties of the Co-30 mass% Cr alloys. The influences of the microstructural features on the mechanical and electrical properties were investigated.

2. Experimental procedure

This work explored various hot-press sintering temperatures and pressures for Co-30 mass% Cr alloys and examined the effects on the microstructure, mechanical properties and electrical behaviors. In this study, 99.95% submicron-structured cobalt (gas-atomized powders) and submicron reduction chromium powders were mixed and underwent hot-press sintering to fabricate the Co-30 mass% Cr alloys. It imposed various hot-press sintering temperatures (1100°C, 1150°C, 1200°C and 1250°C), and pressures (20, 35 and 50MPa) for 1 h, respectively. Meanwhile, the degree of vacuum was maintained at 1.33×10^{-1} Pa. And the specimen size of vacuum hot-press sintering compaction was $40 \times 40 \times 5$ mm^3. A Microtrac X 100 laser was used to analyze the particle size of the submicron-structured powders. Generally speaking, the morphology of gas-atomized powders tends toward an obvious round shape. Moreover, gas-atomized powders possess an excellent forming mechanism and sintering characteristics because the particles have a relatively smooth surface [6,14].

In order to evaluate the sintered behavior of the Co-30 mass% Cr alloys *via* various hot-press sintering temperatures and pressures (the hot pressing apparatus refers to Yu Tai Vacuum Co., Ltd. HPS-1053), the porosity, hardness, transverse rupture strength (TRS) tests, electrical tests and microstructure inspections were performed. Microstructural features of the specimens were examined by X-ray diffraction (XRD, Rigaku D/Max-2200) and scanning electron microscopy (Hitachi-S4700). Porosity tests followed the ASTM B311-08 and C830 standards, and the closed porosity measurement was carried out through the analysis software of Image Pro image. Besides, the sintered density is calculated by the Archimedes Method, and followed the ASTM B311-13 standard [14].

Furthermore, the hardness of the specimens was measured by Rockwell indenter (HRA, Indentec 8150LK) with loading of 588.4 N, which complied with the CNS 2114 Z8003 standard methods. Meanwhile, R_{bm} was the transverse rupture strength (TRS), which determined as the fracture stress in the surface zone. F was maximum fracture load, L was 30 mm, k was chamfer correction factor (normally 1.00-1.02), b and h were 5 mm in the equation $R_{bm} = 3FLk/2bh^2$, respectively. The specimen dimensions of the TRS test were $5 \times 5 \times 40$ mm^3. Moreover, it needs to slightly grind the surface of the specimen and tests at least three pieces. Because CoCr alloys are also used in the thin-film materials, thus the electrical properties are relatively important. Therefore, a four-point probe (LRS4-TG2) was used to measure sheet resistance. In addition, electrical conductivity (σ) was calculated according to the following formula [3,12,14]:

$$\rho = R/t = 1/\sigma$$

Where the ρ is electrical resistivity, R is the resistance, t is the thickness of the test sheet, and σ is the electrical conductivity ($S \cdot cm^{-1}$), respectively.

3. Results and discussion

The morphology of the cobalt and chromium powders is shown in Fig. 1. The morphology of the submicron-size cobalt powders showed more spherical shapes, as shown in Fig. 1a. The mean particle size was 800±45 nm. In addition, the shape of the reduced chromium powders was also spherical with a smooth surface, as shown in Fig. 1b. The mean particle size was about 700±50 nm. Due to the increase in the proportion of cobalt with better ductility, the Co-30 mass% Cr alloys possessed more of the cold welding phenomenon after the planetary ball mill. Simultaneously, The number of revolutions is 300 rpm for 1 h, and the medium is tungsten carbide ball. Most of the ductile and spherical chromium powder particles were coated with cobalt powders (confirmed by the EDS analysis), which showed the irregular shape of the secondary particles, as seen in Fig. 1c.

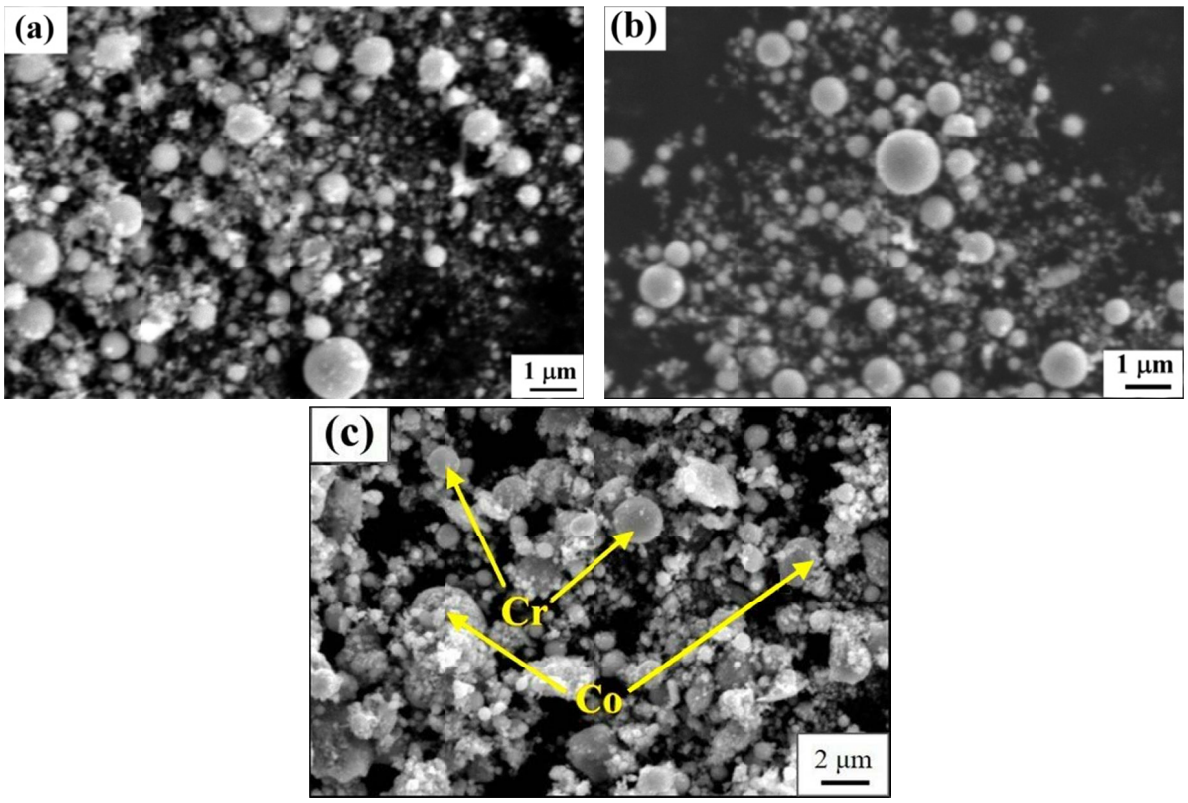

Fig. 1. SEM photographs of the surface morphology: (a) cobalt, (b) chromium powders, and (c) Co-30 mass% Cr alloy powders after 1 h ball mixing, respectively

3.1. Effect of hot-press sintering temperature on microstructural feature

Figure 2a shows the XRD patterns of the Co-30 mass% Cr alloys after the hot-press sintering process at various temperatures. The major diffractions appeared in the Cr (110), FCC structures of Co (111) and (200), and in the HCP structures of Co (100), (101) and (110) planes, respectively. Notably, the Cr_7C_3 peaks were also generated after different temperatures of the hot-press sintering process. Actually, this is related to the hot-press sintering process of this study, which is not in a higher vacuum state. Hence, it is possible to say that the high temperature sintering resulted in the reaction between the chromium and graphite mold, and thus, generated chromium-carbides. Generally, the main densification mechanism of hot-press sintering includes the initial diffusion creep of high temperature and plastic deformation during the hot-press step. When the hot-press entered the sintering stage, the assistance in high compressing stress led to effective plastic deformation and compaction results. Therefore, the Co-30 mass% Cr alloys showed complete diffraction intensity

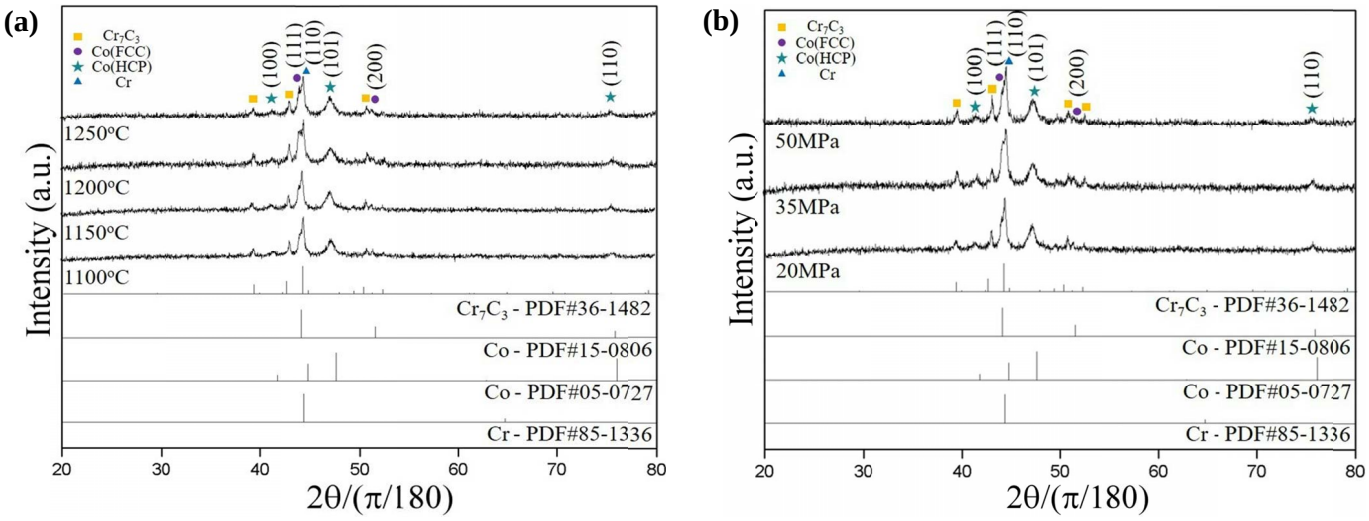

Fig. 2. XRD patterns of Co-30 mass% Cr alloys by hot-press sintering at different (a) temperatures and (b) pressures, respectively

of the Co and Cr phases. As seen in Fig. 2a, these specimens possessed a good crystal structure after hot-press sintering at different temperatures.

Besides, the FCC structure of the cobalt at room temperature is a metastable phase, which is affected easily by external mechanical energy or thermal energy and will become more unstable. Literature has indicated that plastic deformation has led to a large number of defects in the FCC lattices, resulting in constant changes in the lattice and producing the HCP structure of the cobalt.[10] In this work, because the Co-30 mass% Cr alloys possess high contents of cobalt (70 mass%), with the increase in sintering temperature, the Co (111) diffraction plane still maintains a certain intensity. It is reasonable to surmise that the cobalt still retains a certain degree of FCC structure and does not move completely through its martensite transformation into an HCP structure. It can also be found that the FCC structure of Co (200) exists at a higher angle. It is possible to say that the phase transformation (FCC → HCP) seems to not have a significant effect on subsequent sintering behaviors of Co-30 mass% Cr alloys.

As the hot-press sintering temperature increased (1100 → 1150 → 1200 → 1250°C), the Co (111) plane shifted to a slightly lower angle, resulting in a widening and dwarfing phenomenon. This was caused by the FCC structure of cobalt through its martensite transformation into an HCP structure of cobalt. In addition, it is seen that the peaks of Co (100) and Co (101) planes shifted to a lower angle. When the hot-press sintering temperature was increased, there was a more obvious trend toward a low-angle offset phenomenon. This result is caused by the large atomic radius of the chromium (1.28 Å) element generated solid-solution which was transferred into the small HCP structure of cobalt (1.25 Å). It is reasonable to speculate that the increasing temperature effectively enhanced the solid-solution reaction between the cobalt and chromium elements. At the same time, the peak intensity of Cr (110) slightly shifted to a lower angle as the hot-press sintering temperature increased. Hence, it can be concluded that an increase in the temperature of the hot-press sintering effectively increased the lattice diffraction of the unit area and enhanced the relative intensity of Co-30 mass% Cr alloys.

Figure 3 shows the sintered density, apparent porosity, and closed porosity of Co-30 mass% Cr alloys after hot-press sintering at different temperatures. All the detailed data are shown in Table 1. Increasing the temperature of hot-press sintering indeed significantly increased the sintered density and decreased the closed porosity of the specimens. Furthermore, the apparent porosity had a slight declining and rising trend as the temperature of hot-press sintering was increased. The highest sintered density (7.91 g·cm^{-3}) and lowest closed porosities (0.42%) appeared after 1250°C sintering for 1 h. In the present research, the apparent porosity is very low (0.04 ~ 0.11%, as shown in Table 1. It is suitable to suggest that all specimens have reached to near full density (98-99%). In particular, the specimens sintered at 1150°C and 20 MPa for 1 h possessed the appropriate sintered density (7.88 g·cm^{-3}), closed porosities (0.52%), and lowest apparent porosity (0.04%).

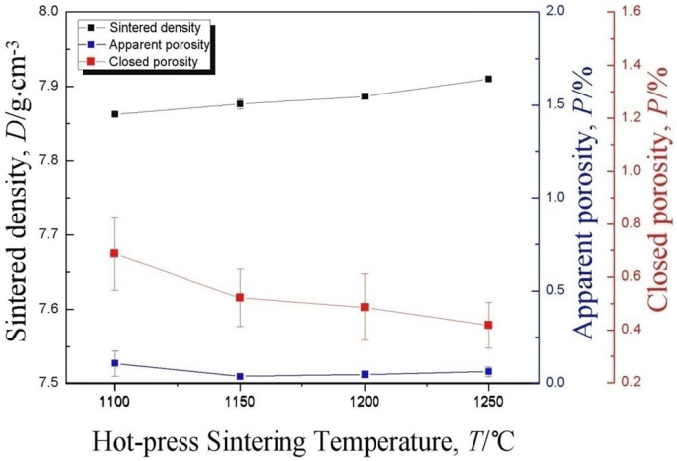

Fig. 3. Comparison of the sintered density, apparent and closed porosities of Co-30 mass% Cr alloys by hot-press sintering at different temperatures

Generally speaking, the melting points were 1495°C for Co and 1907°C for Cr, respectively. Therefore, sintering was carried out in a temperature range of 1100-1250°C where the melting point (T_m) of Cr reached 58-66%. These sintering temperatures were not close to or did not even reach the Cr super-plastic deformation condition (0.6 T_m). Thus, increasing the hot-press sintering temperature (1100 → 1250°C) effectively provided the driving force of the sintering mechanism and helped the atomic diffusion due to external pressure (20 MPa). Furthermore, the submicron-sized particles of the cobalt and chromium powders effectively diffused and filled the pores and increased the contact area between the particles during the high-temperature sintering process. Owing to the Ostwald ripening phenomenon, the large and small pores around the vacancy concentration were different, which easily results in vacancy diffusion, so the small pores become smaller and the large pores become larger [18]. As

TABLE 1

Comparison of the sintered properties and mechanical properties of Co-30 mass% Cr alloys by hot-press sintering at different temperatures

Hot-press Sintering Temperature (°C)	Sintered Density (g·cm^{-3})	Apparent Porosity (%)	Closed Porosity (%)	Mean Grain Size (μm)	Hardness (HRA)	TRS (MPa)
1100	7.86±0.01	0.11±0.07	0.68±0.13	2.14±0.20	76.9±0.4	968.0±2.0
1150	7.88±0.02	0.04±0.01	0.52±0.11	2.33±0.21	77.1±0.2	981.8±8.9
1200	7.89±0.01	0.06±0.02	0.49±0.12	2.82±0.22	75.8±0.4	904.4±20.7
1250	7.91±0.01	0.07±0.03	0.42±0.09	3.87±0.31	75.6±0.5	850.4±22.8

a result, the porosity has an increased and coarsened phenomenon during higher sintering temperatures. This situation most often occurs on the surface of the porosities. Consequently, the apparent porosity slightly increases after 1200°C (0.06%) and 1250°C (0.07%) sintering.

Figure 4 shows the SEM morphology observations of Co-30 mass% Cr specimens after hot-press sintering at different temperatures and pressures. As shown, the white parts are the cobalt grains and the gray parts are the chromium (as indicated by the arrows), respectively. The existence of residual black pores was obvious after hot-press sintering at 1100°C for 1 h, as shown in Fig. 4a. Furthermore, the black pores slightly decreased as the hot-press sintering temperature increased (1150 and 1200°C), as shown in Figs. 4b and 4c. Meanwhile, the high temperature hot-press sintering process led to a grain coarsening phenomenon. As a result, the refined particles of the cobalt and chromium tended to coarsen obviously due to the solid diffusion of the high temperature (1250°C) and high pressure

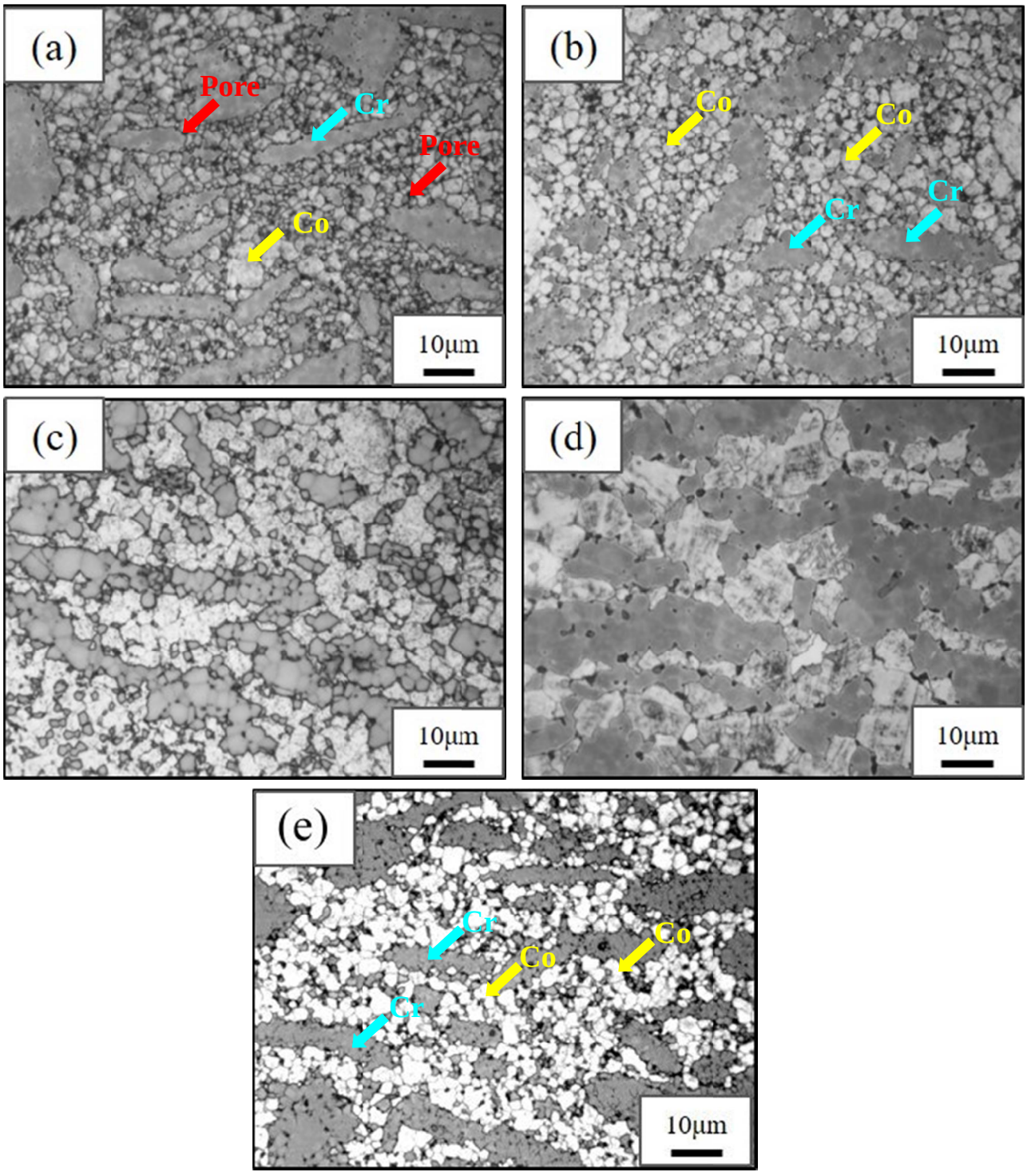

Fig. 4. SEM morphology observations of Co-30 mass% Cr specimens by hot-press sintering at different temperatures and pressures: (a) 1100°C 20 MPa, (b) 1150°C 20 MPa, (c) 1200°C 20 MPa, (d) 1250°C 20 MPa, and (e) 1150°C 50 MPa

(20 MPa), as shown in Fig. 4d. It is clearly found that under the same hot-press pressure (20 MPa), with an increase in sintering temperature, the internal porosity decreases gradually but the grain grows rapidly. Additionally, most of the pores are located in the intergranular (sintering at 1100°C from Fig. 4a), and some of the pores are located in the intergranular (sintering at 1250°C from Fig. 4d). So the pores at the grain boundaries may have a certain inhibitory effect on grain growth.

Figure 4a illustrates the many smaller and randomly dispersed pores in the specimen (closed porosity was 0.68%). These pores possess elliptical and long striped structures. Because of the compaction and solid-phase sintering (SPS) effects of the hot-press pressure, the original pores of the Co-30 mass% Cr alloys gradually decreased, and this led to a lower number of pores. SPS is defined as follows: the shaped compact body is heated to a temperature that is typically 0.5-0.9 of the melting point. No liquid is present and atomic diffusion in the solid state produces a joining of the particles and a reduction of the porosity [14,19]. When the hot-pressed sintering entered the sintering stage (at a sufficiently high temperature), the assistance in high compressive stress led to effective plastic deformation and compaction results. Hence, when the hot-press sintering temperature was increased, the smaller pores slightly decreased in size, as shown in Figs. 4b, 4c, and 4d (closed porosity of 0.52, 0.49, and 0.42%, respectively). The results, when further compared with Fig. 3, revealed that the sintered density gradually increased to 7.91 g·cm^{-3} after hot-press sintering at 1250°C and 20 MPa for 1 h. According to the above discussion and results, a high sintered density and low closed porosities of the Co-30 mass% Cr alloys for SPS were obtained.

Figure 5 reveals the mean grain size of Co-30 mass% Cr alloys after hot-press sintering at different temperatures. In the research, the mean grain size of the Co-30 mass% Cr alloy hot-press sintered specimens was measured using the Linear intercept method [14]. In addition, the literature has indicated that rapid grain growth during the early stage of sintering has been found in many nano and submicron material systems [12,14]. Significantly, the Co-30 mass% Cr alloy powders seemed to lose their submicron-scale characteristics after hot-press sintering, as is often the case for most submicron-size powders, due to the extremely rapid grain growth during high-temperature and high-pressure sintering. However, the mechanism of rapid grain growth needs further examination, especially in the 1250°C sintered specimens.

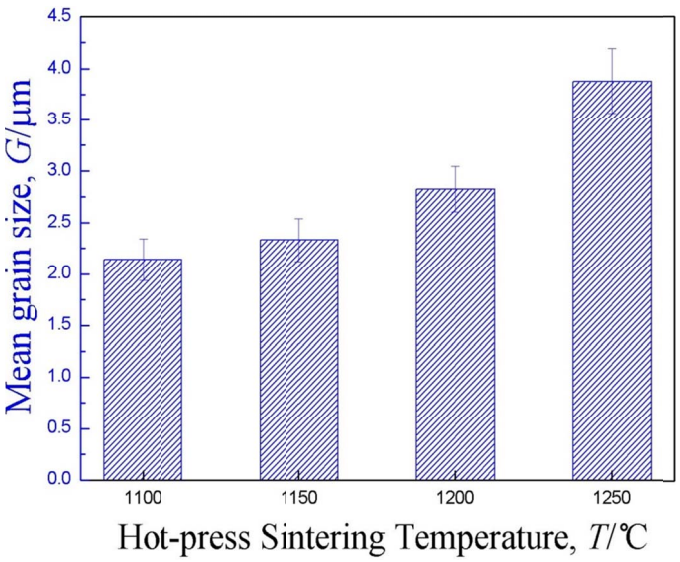

Fig. 5. Comparison of the mean grain size of Co-30 mass% Cr alloys by hot-press sintering at different temperatures

With the increase in hot-press sintering temperatures (1100 → 1150 → 1200 → 1250°C), the mean grain size gradually increased (2.14 → 2.33 → 2.82 → 3.87 μm), as shown in Table 1. The grain coarsening phenomenon slightly appeared in the Co-30 mass% Cr alloy hot-press sintered specimens, especially for hot pressing temperature that increased from 1200°C to 1250°C. These results are consistent with those shown in Fig. 4. Additionally, our previous studies [12,14,15] also confirmed that rapid grain growth during the early stage of sintering has been found in many submicron material systems. In general, extremely rapid grain growth was readily generated during high-temperature and high-pressure sintering. Although the 1250°C sintering specimens have higher sintered density and a lower closed porosity, the grain coarsening phenomenon will affect the subsequent mechanical property tests. Consequently, grain growth creates an impact on the mechanical properties of the hot-press sintered Co-30 mass% Cr alloy.

3.2. Effect of the hot-press sintering temperature on TRS and hardness

Figure 6a presents the TRS and hardness tests of Co-30 mass% Cr alloys by hot-press sintering at different temperatures (the detailed data is also shown in Table 1). The highest TRS (981.8 MPa) and hardness (77.1 HRA) values appeared after 1150°C hot-press sintering and 20 MPa for 1 h. In this work, the significantly grain coarsening phenomenon appeared in the 1200 and 1250°C-sintered specimens (Fig. 4), which was disadvantageous to the strength and hardness. Thus, the specimens possessed a lower TRS and hardness value (Fig. 6a) after sintering at 1200 and 1250°C. Clearly, the results show that the coarsening phenomenon of the Co-30 mass% Cr alloys had a corresponding relationship with the TRS.

In this study, increasing the hot-press sintering temperature (1100 → 1250°C) slightly improved the sintered density (7.86 → 7.91 g·cm^{-3}) of the Co-30 mass% Cr alloys. In spite of the closed pores obviously decreasing (0.68% → 0.42%) the grain size coarsening phenomenon seems to be an important factor affecting the TRS values. According to the Hall-Petch equation, the mechanical strength of the materials decreased with the coarsening of the grain [20,21], and a significant decrease in strength appeared at 1200 and 1250°C. The results agree with the SEM observation and mean grain size tests, as shown in Figs. 4 and 5. In addition, as the hot-press sintering temperature increased up to 1200°C, the FCC structure of the cobalt went through its martensite transformation into an HCP structure of

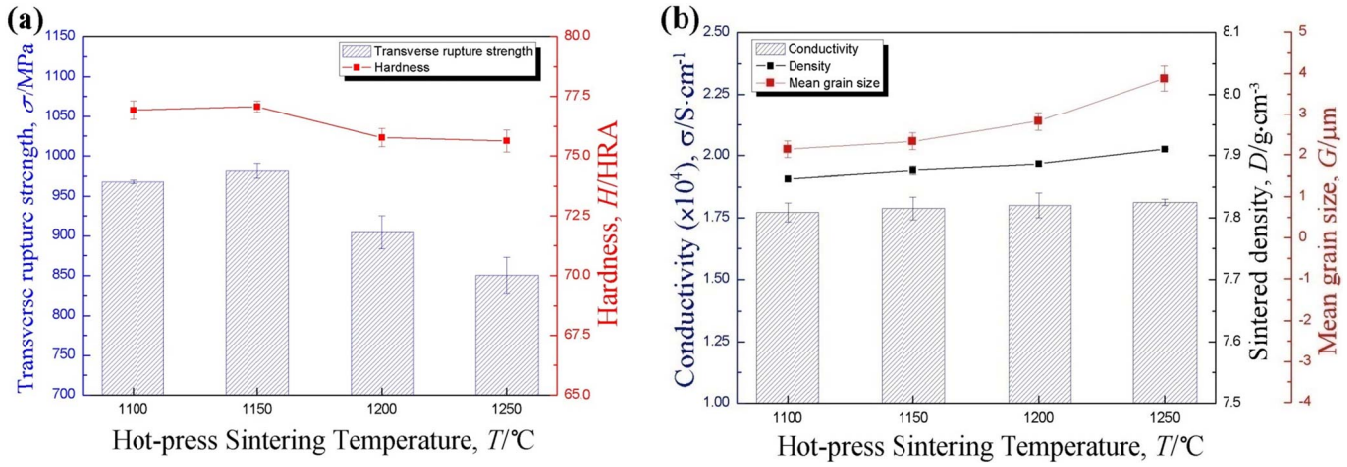

Fig. 6. Comparison of the mechanical and electrical tests of Co-30 mass% Cr alloys by hot-press sintering at different temperatures: (a) TRS and hardness tests, and (b) conductivity test

cobalt (see the Fig. 2). As a result, this caused the sliding system to be reduced and led to the decrease in the plastic deformation (brittle rupture) of the Co-30 mass% Cr alloys. This is why the TRS displayed obvious decrease after sintering at 1250°C. Apparently, grain growth plays an important role in affecting the TRS value. Moreover, the phase transformation of cobalt could also be another factor causing a decrease in the TRS value.

Figure 6a also indicates that the hardness values of the Co-30 mass% Cr alloys have a similar trend with TRS for the different sintering temperatures. Previous studies revealed that decreasing the porosities of the hot-press sintered materials effectively enhanced the plastic deformation resistance and hardness [3,12,14]. Although the closed pores decreased as the hot-press sintering temperature increased, as mentioned previously, the grain growth and grain size coarsening phenomenon still resulted in the hardness values declining after hot-press sintering at 1200 and 1250°C for 1 h. Consequently, the highest hardness value (77.1 HRA) appeared in 1150°C-sintered specimens. As the hot-press sintering temperature increased to 1200 and 1250°C, the hardness values gradually decreased to 75.8 and 75.6 HRA, respectively. According to above the discussion and results, it is reasonable to conclude that the grain size and SPS processes resulted in the differences in the mechanical property tests (hardness and TRS).

Figure 7 shows the fractographic observations of Co-30 mass% Cr alloys after hot-press sintering at different temperatures. As seen in Fig. 7a, residual pores clearly existed in the fracture surface, as indicated by the arrows. These pores generated the stress concentration point and resulted in the source of crack propagation. As the sintering temperature was increased (1100 → 1150 → 1200 → 1250°C), the number of residual pores slightly decreased, as shown in Figs. 7b-7d. But the grain size was obviously increased. In particular, the 1250°C sintered specimens possessed significant coarse grains, thus, a lot of cleavage fractures appeared and resulted in the lowest TRS value (850.4 MPa), as shown in Fig. 7d. In addition, Co-30 mass% Cr alloys possess higher Co content. The fractographs show that some ductile and brittle fractures coexisted in the Co-30 mass% Cr alloys after the TRS tests. In other words, when the deformation of a specimen exceeds its own limit, it will crack directly from the stress concentration. This causes the local chromium particles near the Co-Cr interfaces to spread and expand rapidly, which is detrimental to the fracture resistance of the interface. The general aspect of the fracture showed dimpled ruptures and small cleavages [22,23]. As a result, many dimple fractures clearly existed in the rupture surface which resulted in the higher TRS value (981.8 MPa), as shown in Fig. 6a. On the other hand, the fracture mechanism was evidenced by the brittle chromium generating cleavage and transgranular fractures, as indicated by the arrows shown in Fig. 7d.

Figure 8 shows the high-magnification fractograph of Co-30 mass% Cr specimens after 1250°C sintering for 1 h. After further observation and analysis, the rupture morphology of 1250°C sintered specimens showed cleavage steps of the transgranular fracture which were formed by the intersection of two different heights of the fracture surface and show a similar river direction. Because the grain size was relatively small (3.87 μm), it did not form river-like stripes. Significantly, the cleavage steps of the transgranular fracture existed in the high temperature sintered Co-30 mass% Cr alloys that caused lower TRS values.

3.3. Effect of the hot-press sintering temperature on electrical performance

Figure 6b show the conductivity, sintered density, and mean grain size of the Co-30 mass% Cr alloys after hot-press sintering at different temperatures. The electrical performance, sintered density, and mean grain size of the sintered Co-30 mass% Cr alloys exhibited a positive tendency. When the hot-press sintering temperature was increased, the sintered density and mean grain size obviously increased, and the electrical conductivity revealed an upward trend ($1.77 \rightarrow 1.79 \rightarrow 1.80 \rightarrow 1.81 \times 10^4$ S·cm^{-1}). However, the difference was not obvious. Particularly, as the sintering temperature increased to 1250°C, the grain size rapidly grew but the conductivity still increased slowly. The grain coars-

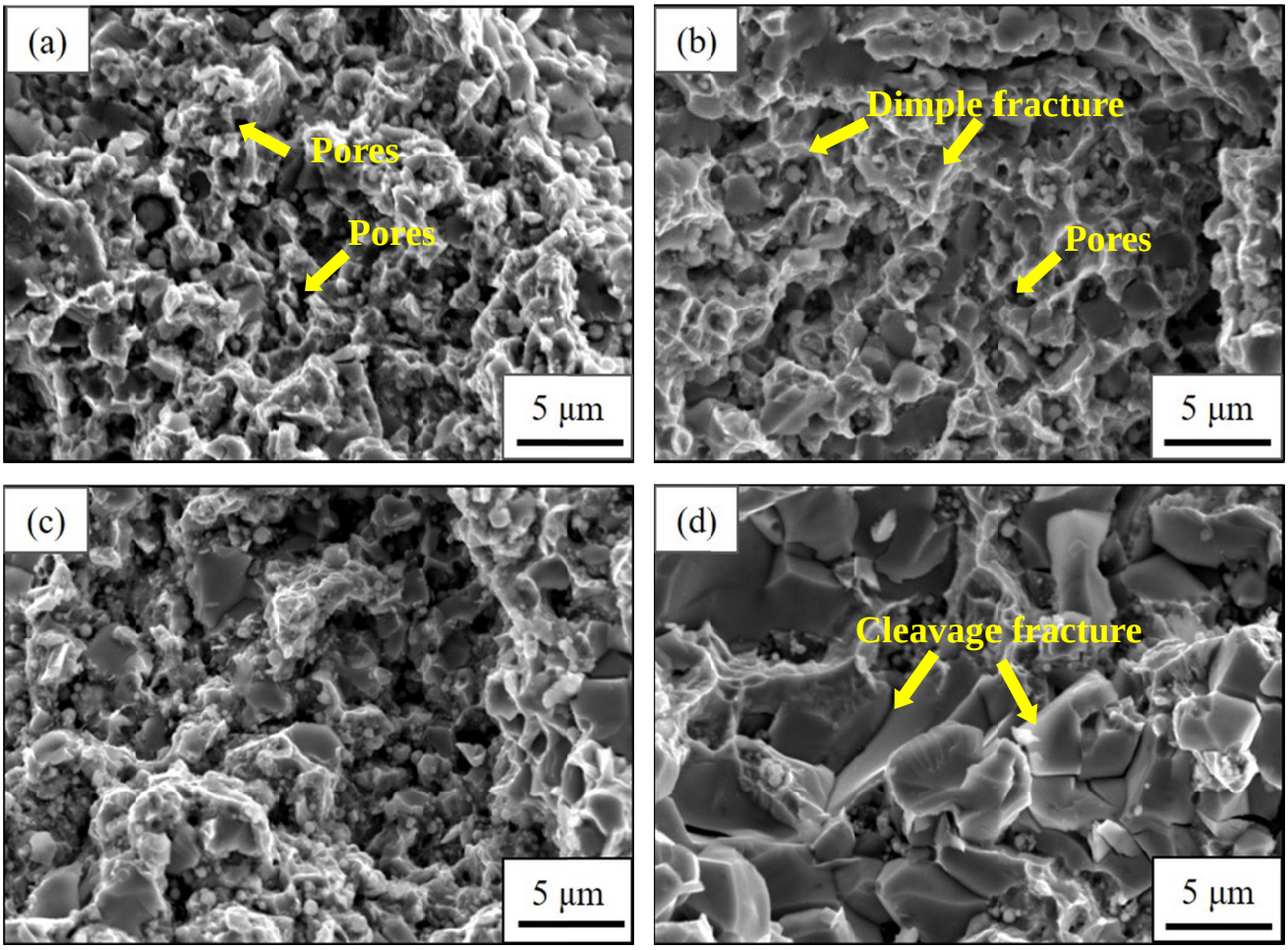

Fig. 7. Fractographs observation of Co-30 mass% Cr specimens by hot-press sintering at different temperatures: (a) 1100°C, (b) 1150°C, (c) 1200°C, and (d) 1250°C

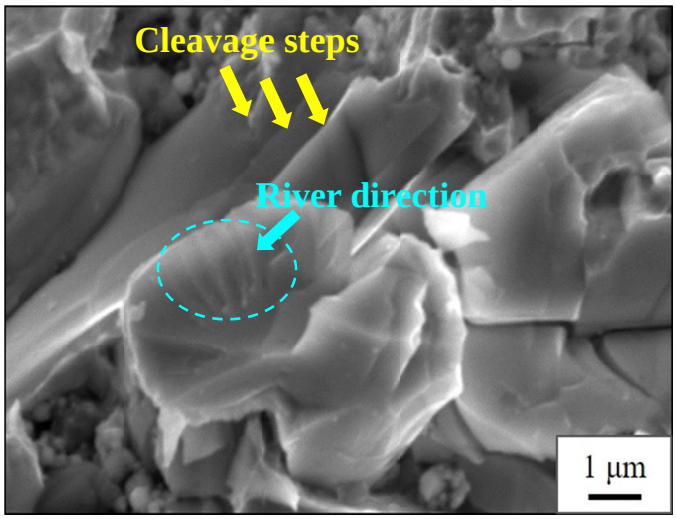

Fig. 8. High-magnification fractograph of Co-30 mass% Cr specimens after 1250°C sintering for 1 h

ening results in the grain boundary showed a decrease. Grain boundaries are crystallographic defects in the crystal structure and tend to decrease the electrical conductivity of the material. The bigger grain size allows the electrons in the alloy to migrate with less energy barrier. In addition, our previous studies also indicated a relationship between the sintered density of Cr-based alloys and the electrical properties [3,12,14]. Increasing the sintered density obviously improved the electrical properties of the Cr-based alloys. As the number of internal residual pores decreased, the free electrons in the process were able to move because of fewer obstacles. Then, the higher sintered density and lower porosity led to an increase in the mean free path of the electrons, which improved electrical performance.

In this study, the sintered density was clearly enhanced after the high-temperature hot-press sintering process (7.86 → 7.91 $g \cdot cm^{-3}$), which is advantageous to the electrical properties of hot-press sintered Co-30 mass% Cr alloys. On the other hand, although increasing sintering temperatures seems to slightly improve the martensite transformation of cobalt in high cobalt content alloys, the migration of electrons within the alloys can possibly be restricted. Consequently, the electrical properties of the hot-press sintered Co-30 mass% Cr alloys are slightly improved as the sintering temperature increased. From the discussion and results above it can be seen that the hot-press sintering parameters of 1150°C at 20 MPa for 1 h for the Co-30 mass% Cr alloys obviously possess optimal mechanical properties and suitable electrical conductivity.

3.4. Effect of the hot-press sintering pressures on the Co-30 mass% Cr alloys

In order to further understand the effect of hot-press sintering pressures on the Co-30 mass% Cr alloys, the following study imposes various hot-press sintering pressures (20, 35 and 50 MPa) while maintaining the sintering temperature at 1150°C for 1 h, respectively. Fig. 2b shows the XRD patterns of Co-30 mass% Cr alloys after the hot-press sintering process at various pressures. Similarly, the major diffractions appeared in the Cr (110), FCC structures of Co (111) and (200), and in the HCP structures of Co (100), (101) and (110) planes, respectively. The Cr_7C_3 peaks were also generated after different pressures of the hot-press sintering process. As the pressure increased (20 → 35 → 50 MPa), the intensity of the Cr diffractions (110) slightly increased. Significantly, increasing the hot-press pressure served to slightly increase the intensity of Co and Cr phases, and effectively enhance the overall crystallinity, further improving the microstructures and properties of the Co-30 mass% Cr alloys. This result also reveals that the increasing the hot-pressing sintering pressure at a lower temperature (1150°C), which can achieve the similar sintering effect at a higher sintering temperature and lower pressure.

Table 2 shows the sintered properties and mechanical properties of Co-30 mass% Cr alloys by hot-press sintering at different pressures. In this work, the highest sintered density (7.95 $g \cdot cm^{-3}$) appeared after hot-press sintering at 1150°C, 50 MPa for 1 h; while the lowest apparent porosity (0.02%) and closed porosity (0.39%) were also produced. Clearly, the apparent porosities and closed porosities obviously declined as the pressure of the hot-press sintering increased. Actually, in the final stage of hot-press sintering the porosity should be eliminated. It is reasonable to speculate that the sintering densities of the Co-30 mass% Cr alloys increased mainly due to the tight compaction of the relatively ductile cobalt particles via the enhanced pressure. Fig. 4e shows the SEM morphology observations of Co-30 mass% Cr specimens after hot-press sintering at 1150°C, 50 MPa for 1 h. It can be observed that the shape of the chromium phase grains changes, and it exhibits the same elongated shape as the direction in which the hot-pressing pressure is applied. This result shows that the higher hot-pressing pressure (50 MPa) can transfer energy more effectively, which resulting in an obvious plastic strain, and then to improve mechanical properties.

Further comparison of the average grain sizes of the Co-30 mass% Cr alloys by hot-press sintering at different pressures is shown in Table 2. The average grain size was measured using the linear intercept method [14].As the hot-press sintering pressure increased, the average grain size gradually increased (2.33 → 2.45 → 2.50 μm). Generally speaking, grain growth always has an impact on the mechanical properties of the material. However, the grain coarsening phenomenon did not clearly appear in the Co-30 mass% Cr alloys after high-pressure hot-press sintering; the actual increase in grain size was only 0.17 μm (2.33 → 2.50 μm). It is possible to say that increasing the pressure contributes to the diffusion of atoms, which can shorten the time of entry into the late sintering, and thus, quickly achieve the sintering of the densification mechanism.

Table 2 also revealed the TRS and hardness tests of the Co-30 mass% Cr alloys by hot-press sintering at different pressures. As the hot-press sintering pressure increased, the higher sintered density provided stronger binding to prevent the rupture mechanism of generation. In the research, increasing the pressures of the hot-press sintering obviously enhanced the sintered density (7.88 → 7.92 → 7.95 $g \cdot cm^{-1}$) of the Co-30 mass% Cr alloys. As a result, the higher bonding strength then hindered the generation of the rupture mechanism. The TRS values showed an increasing trend and slight decline (981.8 → 997.1 → 974.8 MPa) as the hot-press sintering pressure increased. It is reasonable to suggest that the average grain sizes of coarsening phenomenon (2.33 → 2.50 μm) seems to play an important effect.

The hardness values of the Co-30 mass% Cr alloys showed a slight enhanced as the hot-press sintering pressure increased, as shown in Table 2. In the present work, the levels of apparent porosity and closed porosity were under 1% after the hot-press sintering at different pressures. As the pressure increased (20 → 50 MPa), the change in hardness values went from 77.1 to 77.6 HRA. Our previous studies revealed that decreasing the porosities of the sintered materials effectively enhanced plastic deformation resistance and hardness [12,14,15]. According to above the discussion and results, hot-press sintering parameters of 1150°C at 35 MPa for 1 h for the Co-30 mass% Cr alloys obviously possessed optimal properties. Consequently, hot-press sintering is a really practical method to obtain Co-30 mass% Cr alloys with good microstructure and mechanical properties.

4. Conclusion

In the present research, it was found that the optimal temperature parameters of the hot-press sintered Co-30 mass% Cr alloys are 1150°C sintering at 20 MPa for 1 h. Meanwhile, the electrical conductivity was about 1.79×10^4 $S \cdot cm^{-1}$, and the hard-

TABLE 2

Comparison of the sintered properties and mechanical properties of Co-30 mass% Cr alloys by hot-press sintering at different pressures

Hot-press Sintering Pressure (MPa)	Sintered Density ($g \cdot cm^{-3}$)	Apparent Porosity (%)	Closed Porosity (%)	Mean Grain Size (μm)	Hardness (HRA)	TRS (MPa)
20	7.88±0.02	0.04±0.01	0.52±0.11	2.33±0.21	77.1±0.20	981.8±8.90
35	7.92±0.02	0.03±0.01	0.46±0.08	2.45±0.23	77.2±0.30	997.1±17.4
50	7.95±0.03	0.02±0.01	0.39±0.09	2.50±0.19	77.6±0.31	974.8±14.4

ness and TRS reached 77.1 HRA and 981.8 MPa, respectively. The 1150°C-sintered Co-30 mass% Cr alloys also possessed the optimal SPS results (lowest apparent porosity of 0.04% and appropriate mean grain size of 2.33 μm).

Increasing the temperature of the hot-press sintering is effective in increasing the lattice diffraction of the unit area and enhancing the relative intensity of Co-30 mass% Cr alloys. As the sintering temperature was increased, the intensity of the Cr (110) planes increased obviously. However, the cobalt still retained a certain degree of FCC structure; it did not move completely through its martensite transformation into an HCP structure. Consequently, the phase transformation (FCC → HCP) of cobalt does not have a significant effect on subsequent sintering behaviors of Co-30 mass% Cr alloys. Additionally, the high temperature hot-press sintering of grain growth plays an important role in affecting the mechanical property, while the phase transformation of cobalt also slightly affects the sintered results.

Increasing the hot-press pressure effectively enhance the overall crystallinity, further improving the microstructures and properties of the Co-30 mass% Cr alloys. It is possible to conclude that the hot-press sintering parameters of 1150°C at 35 MPa for 1 h for the Co-30 mass% Cr alloys obviously possessed optimal mechanical properties. Simultaneously, the sintered density reached 7.92 $g \cdot cm^{-3}$, the closed porosity was 0.46%, the hardness and TRS reached 77.2 HRA and 997.1 MPa, respectively.

Acknowledgments

This research is supported by the ASSAB STEELS TAIWAN CO., LTD. The authors would like to express their appreciation for Dr. Harvard Chen, Michael Liao and Mr. Meng-Yu Liu.

REFERENCE

[1] J.A. García, C. Díaz, S. Mändl, J. Lutz, R. Martínez, R.J. Rodríguez, Surface and Coatings Technology **204**, 2928-2932 (2010).
[2] G.J. Cui, J.R. Han, G.X. Wu, Wear **346-347**, 116-123 (2016).
[3] S.H. Chang, C.L. Liao, K.T. Huang, M.W. Wu, Materials Transactions **57**, 732-737 (2016).
[4] G. Khatibi, M. Lederer, A. B. Kotas, M. Frotscher, A. Krause, S. Poehlmann, International Journal of Fatigue **80**, 103-112 (2015).
[5] S. Mändl, C. Díaz, J .W. Gerlach, J.A. García, Nuclear Instruments and Methods in Physics Research Section B: Beam Interactions with Materials and Atoms **307**, 305-309 (2013).
[6] J. Lutz, C. Díazc, J.A. García, C. Blawert, S. Mändl, Surface and Coatings Technoloy **205**, 3043-3049 (2011).
[7] A. Galdikas, A. Petraitienė, T. Moskalioviene, Vacuum **119**, 233-238 (2015).
[8] R. Bhure, A. Mahapatro, C. Bonner, T.M. Abdel-Fattah, Materials Science and Engineering C **33**, 2050-2058 (2013).
[9] H.R. Kim, Y. K. Kim, J.S. Son, B.K. Min, K.H. Kim, T.Y. Kwon, Materials Letters **178**, 300-303 (2016).
[10] J.A. Betancourt-Cantera, F. Sánchez-De Jesús, G. Torres-Villaseñor, A.M. Bolarín-Miró, C.A. Cortés-Escobedo, Journal of Alloys and Compounds **529**, 58-62 (2012).
[11] S.H. Chang, P.Y. Chang, Materials Science and Engineering A **606**, 150-156 (2014).
[12] S.H. Chang, C. Liang, J.R. Huang, K.T. Huang, Powder Metallurgy **59**, 142-147 (2016) .
[13] A.K. Shukla, S.V.S. Narayana Murty, R.S. Kumar, K. Mondal, Journal of Alloys and Compounds **580**, 427-432 (2013).
[14] S.H. Chang, C.L. Li, K.T. Huang, Materials Transaction **58**, 1190-1196 (2017).
[15] S.H. Chang, P.Y. Chang, Materials Science and Engineering A **618**, 56-62 (2014).
[16] B. Henriques, A. Bagheri, M. Gasik, J.C.M. Souza, O. Carvalho, F.S. Silva, R.M. Nascimento, Materials & Design **83**, 829-834 (2015).
[17] Y. Sato, N. Nomura, S. Fujinuma, A. Chiba, Journal of Japan Institute Metals **72**, 532-537 (2008).
[18] A. Baldan, Journal of Materials Science **37**, 2171-2202 (2002).
[19] W.D. Kingery, M. Berg, Journal of Applied Physics **26**, 1205-1212 (1955).
[20] E.O. Hall, Proceedings of the Physical Society. Section B **64**, 747-753 (1951).
[21] N.J. Petch, Journal of the Iron and Steel Institute **174**, 25-28 (1953).
[22] K.T. Huang, S.H. Chang, P.C. Hsieh, Journal of Alloys and Compounds **712**, 760-767 (2017).
[23] S.H. Chang, P.T. Yeh, K.T. Huang, Vacuum **142**, 123-130 (2017).